Effect of Water Hardness Ions on the Solution Properties of an Anionic Surfactant

P.C. Hu* and **M.E. Tuvell**
Ethyl Corp., Ethyl Technical Center, P.O. Box 14799, Baton Rouge, LA 70898

The solution characteristics of the system linear alkylbenzene sulfonate (LAS)/Ca^{++}/builder were studied using a dynamic surface tension technique. The results showed that the rate of CA^{++}/LAS interaction is slower than the CA^{++} binding rate of zeolite A. Consequently, zeolite A is effective in preventing precipitation of LAS by calcium ions. The data obtained from the study of Ca^{++} binding detergent builders on solubilization of $Ca(LAS)_2$ showed that zeolite A was effective but the rate of solubilization was much slower than that for STPP. Incorporation of a small amount of phosphate with zeolite A in a detergent significantly increases the rate of solubilizing of $Ca(LAS)_2$.

The amount of surfactant that can be absorbed at a rapidly created gas/liquid interface is related to the concentration of the surfactant in the liquid. The concentration of the surfactant in the liquid depends, in turn, upon the interaction between surfactant and water hardness ions as well as the electrolyte concentration. The approach used to study the interaction between an anionic surfactant and inorganic cations in the solution in this investigation was to monitor the adsorption of surfactant at a rapidly created surface as indicated by the value of the dynamic surface tension. Because the transport of a surfactant molecule from the bulk of a solution to a gas/liquid interface is much faster than the interaction between surfactant and water hardness ions, the method is suitable for obtaining kinetic information relating to the interaction of anionic surfactants with hardness ions.

A dynamic surface tension method (1) was used to evaluate the effectiveness of various detergent builders in protecting LAS from calcium ions.

INSTRUMENTATION AND EXPERIMENTAL PROCEDURE

The maximum bubble pressure apparatus consisted of a gas feeding system, a pressure measuring system and a foam evaluation system. The gas feeding system consisted of a pressure regulator, a mass flow meter, a mechanical flow control valve and a flow control unit allowing a steady, preselected volume of gas to be delivered to the capillary to facilitate foam generation. The pressure variation in the capillary during a bubble formation was monitored by a pressure transducer. The output from the pressure transducer was fed into a demodulator and then directed into an oscilloscope and a strip chart recorder. The oscilloscope was used to obtain pressure information generated at very high bubble formation rates where the response of the chart recorder was too slow. The foam evaluation system consisted of a magnetic stirrer and a jacketed column equipped with a bottom drain valve and a capillary port; it allowed different sized capillaries to be introduced into the column to generate foams of specific and well-defined cell size.

As gas flows through a capillary tube immersed under the surface of a liquid at a depth of h, the radius of the liquid/gas interface formed at the tip of the capillary is related to the gas phase pressure, P, by the Laplace equation. P reaches a maximum, Pmax, when the radius of the bubble decreases to the radius of the capillary used.

$$Pmax = P\text{-}Po = 2\sigma/R + \varrho gh$$

Where Po is the atmospheric pressure, σ is the surface tension, R is the radius of the capillary, ϱ is the density of the liquid and g is the acceleration of gravity.

At the beginning of a measurement, the liquid level was raised until the tip of the chlorotrimethylsilane-treated capillary just touched the air/liquid interface and $P^T max$ was measured. At this condition, the hydraulic pressure is zero. Therefore, $P^T max$ is proportional to the surface tension by the factor of 2/R. The superscript "T" denotes that the capillary just touches the surface of the liquid. After determining $P^T max$ the liquid was raised to immerse the tip of the capillary below the surface and Pmax was recorded at the same bubbling rate. The difference between Pmax measured with the capillary immersed and $P^T max$ is the hydraulic pressure of immersion ϱgh. An arbitrary but constant immersion depth of 6.3 mm to give a response of 100 mV increase in the pressure transducer reading was used throughout this work.

After ϱgh was established, the nitrogen feeding rate was then either varied to establish the relationship between surface tension and bubble formation rate (surface aging) or adjusted to monitor the interactions between a linear alkylbenzene sulfonate and electrolyte using a constant bubble formation rate of three sec/bubble. The radius of the capillary used was 0.0238 cm. The sensitivity of the equipment was such that one mV corresponded to about 0.0735 erg/cm^2.

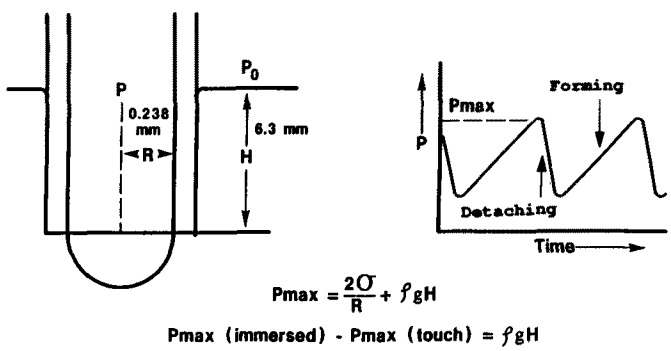

FIG. 1. Maximum bubble pressure method.

*To whom correspondence should be addressed.

Dynamic surface tension is the surface tension of a freshly created surface measured during expansion and represents a nonequilibrium state (2). As illustrated in Figure 1, a bubble cycle can be visualized as a two-step process: (i) a bubble forming step and (ii) a bubble-detaching step. The bubble-detaching step requires about 4×10^{-2} seconds to complete. When the bubble-detaching time is insignificant relative to the time of the complete bubble cycle, the bubble formation rate is directly proportional to the expansion rate of gas/liquid interface or the rate of stretching of the surface. At very high bubble formation rates, approaching that required for bubble detachment, the bubble formation rate is no longer adequate to describe the stretching rate of the gas/liquid interfaces.

For the foam stability study, the foam was generated at a gas flow rate of 120 cm^3/min. The foam column measured 2.54 cm in radius and 100 cm in height. The foam column was thermostated to 23 C. Foam generated under these conditions which reached a steady state height greater than 100 cm was considered "stable." If the steady state foam height was less than 100 cm, the foam was considered to be "unstable." When the steady state foam height reached a height of 100 cm, the gas flow was stopped and foam height was monitored as a function of time.

RESULTS AND DISCUSSION

Figure 2 shows the variation of dynamic surface tension with the bubble generation rate for various concentrations of a commercial linear alkylbenzene sulfonate (LAS). The range of bubble generation rates investigated was from 10 sec/bubble to 6×10^{-2} sec/bubble. The relationship between the dynamic surface tension and the rate of bubble formation is shown as a family of curves with each curve representing a given surfactant concentration. As expected, at a given concentration the dynamic surface tension measured at a high rate of bubble formation (short surface aging) is always higher than that measured at a lower rate of bubble (surface) formation. Also as expected, at a high rate of bubble formation and low surfactant concentration, the dynamic surface tension approaches that of pure water, 72 erg/cm^2. At surfactant concentrations substantially higher than the CMC and at a sufficiently low rate of surface formation, the rate of adsorption of surfactant into the newly created surface is sufficient to attain an equilibrium state (3,4). Under these conditions, the dynamic surface tension is the surface tension of the solution. At any given rate of bubble formation, higher dynamic surface tensions are observed at lower surfactant concentrations. In addition, the data also show that the dynamic surface tension is more sensitive to variations in surfactant concentration than the equilibrium surface tension.

Figure 3 is a semi-logarithmic plot of the dynamic surface tension measured at a rate of bubble formation of 10 sec/bubble as a function of surfactant concentration. Based on this plot the CMC is 0.4 g/l or 1.1×10^{-3} mol/l. A continuous decrease in the dynamic surface tension is observed at surfactant concentrations well above CMC. The data of Figure 4 illustrate that for any given rate of bubble formation, adding the

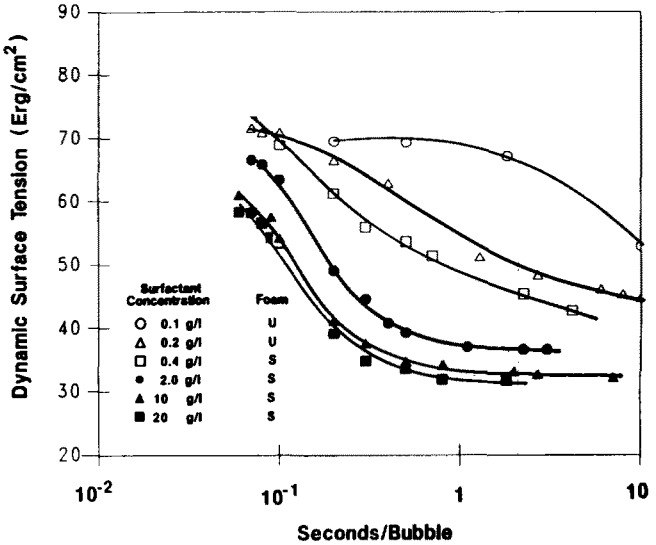

FIG. 2. Dynamic surface tension as a function of surfactant concentrations. S, stable foam, and U, unstable foam.

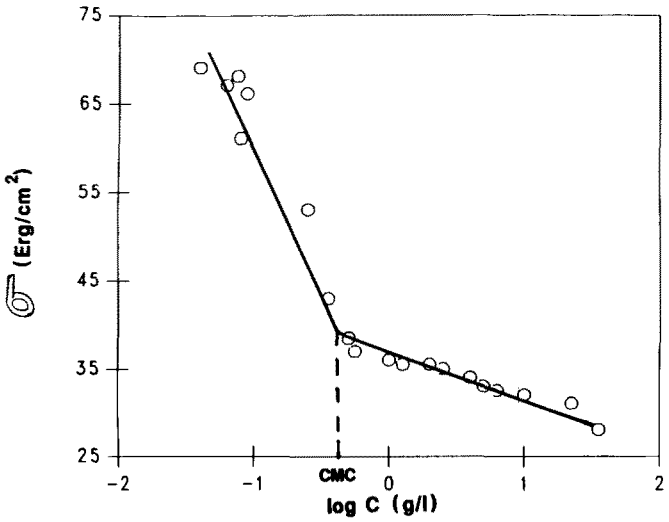

FIG. 3. Dynamic surface tension (measured at 10 sec/bubble) as a function of surfactant concentration.

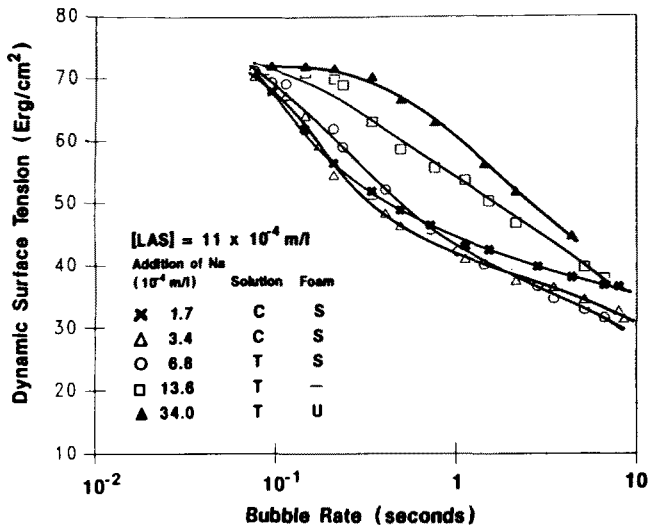

FIG. 4. Dynamic surface tension as a function of Na^+ concentration. S, stable foam; U, unstable foam; C, clear solution, and T, turbid solution.

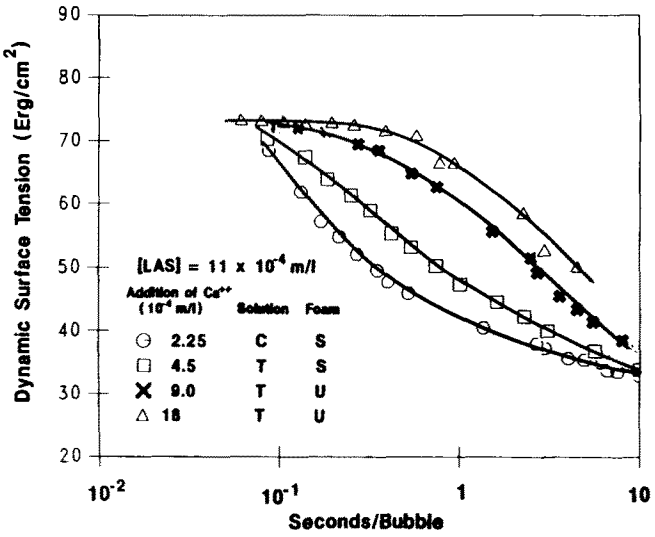

FIG. 5. Dynamic surface tension as a function of C^{++} concentration s.

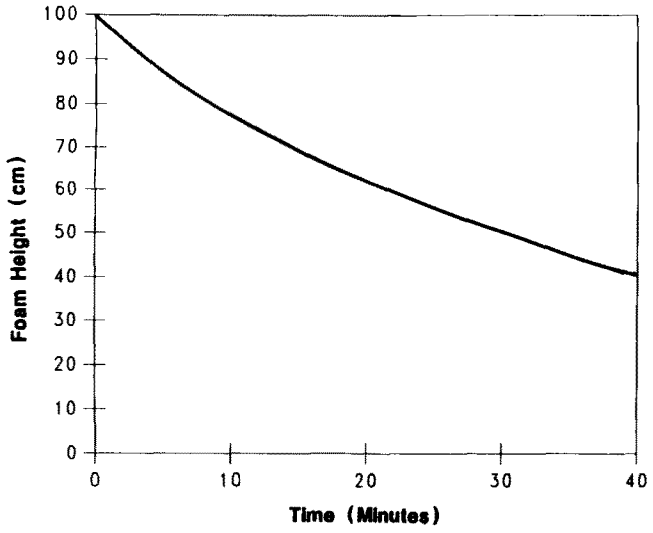

FIG. 6. Foam stability.

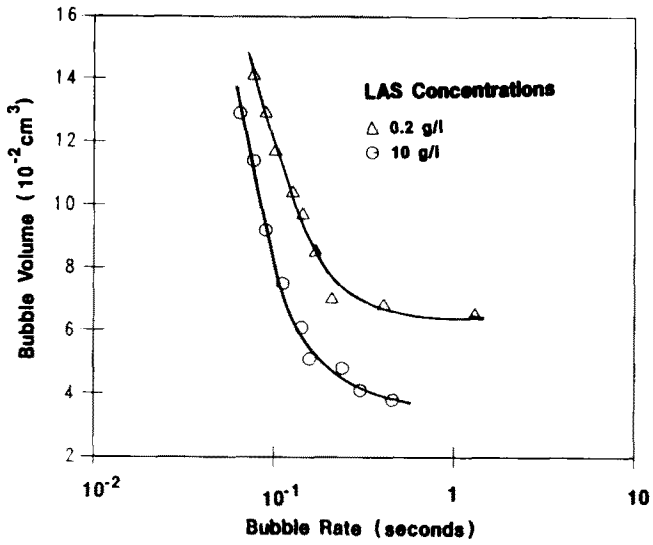

FIG. 7. A comparison of foam cell size.

electrolyte sodium chloride at concentrations up to 3.4 $\times$ 10^{-4} mol/l resulted in corresponding decreases in dynamic surface tensions. Further increases in sodium chloride concentration resulted in the solution becoming cloudy between 3.4 $\times$ 10^{-4} and 6.8 $\times$ 10^{-4} mol/l. The dynamic surface tension started to increase as the solution became turbid. The variation in electrolyte concentration had little affect on the dynamic surface tension at very high and very low rates of bubble formation. Observation of the corresponding foaming characteristics showed an abrupt decrease in foam stability coinciding with the change in the shape of the curves from concave to convex. This suggests that more stable foams are formed under conditions where the rate of adsorption of the surfactant at the interface is faster.

The data represented by Figure 5 were generated under conditions similar to those used for Figure 4 with the exception that calcium chloride was used as the electrolyte instead of sodium chloride. It was observed that at low Ca^{++} concentrations, the dynamic surface tension was reduced while at higher Ca^{++} concentrations $Ca(LAS)_2$ precipitated and the dynamic surface tension increased. Again, observation of corresponding foam characteristics showed an abrupt decrease in the foam stability coinciding with the curves being concave or convex. The inflection in the shape of the curves from convex to concave does not coincide with solution turbidity. On an equal molar basis, the dynamic surface tension was observed to be much more sensitive to the presence of calcium ions than sodium ions.

It was found that foams of 100 cm or more in height had the same decay pattern as shown by Figure 6. The foam decay patterns were generated using five different LAS concentrations in the range of 0.4 g/l to 20 g/l. Of the foams classified as "unstable," none reached a steady state height greater than 50 cm and none had a consistently uniform foam structure. The decay pattern of these "unstable" foams could not be monitored.

As mentioned earlier, the volume of gas flowing through the capillary was controlled using a mass flow meter. Consequently, the volume of the bubble formed can be calculated from the mass flow rate and the corresponding bubble formation rate. Figure 7 is a plot of the bubble volume as a function of rate of bubble formation for surfactant solutions of 0.2 g/l and 10 g/l concentrations, respectively. As expected, for a given bubble formation rate, finer foam cell sizes were formed at the higher surfactant concentration. In addition, the size of the foam cell generated was observed to be determined by the bubble formation rate.

The maximum bubble pressure method of determining dynamic surface tension was used to study the effectiveness of various detergent builders for protecting anionic surfactant from calcium interaction. The experimental procedure can be illustrated by inspection of Figure 8. This figure is a copy of the strip chart recording of a maximum bubble pressure dynamic surface tension measurement. Starting from the left, the tip of the capillary was touching the surface of the surfactant solution with gas flowing at a rate of three sec/bubble. The recorder was set at a chart speed of

one inch/min. The chart speed was then increased to 10″/min to examine the actual bubble formation cycle. Under these conditions, the bubble detaching time is insignificant relative to the time required to complete a bubble cycle. The chart speed was then reduced back to one inch/min and the tip of the capillary was immersed to such a depth that a 100-MV response was received from the pressure transducer. When agitation was provided by a magnetic bar at a constant rotation speed of 60 RPM, a Vortex was generated which reduced the hydraulic pressure at the capillary tip and resulted in an increase in the bubble formation rate. To compensate for this, the nitrogen feed rate was reduced such that the original bubble formation rate of three sec/bubble was obtained. The variation of dynamic surface tension measured at three sec/bubble was used to monitor the interaction between LAS and Ca^{++}.

The data represented by Figure 9 showing the dynamic surface tension as a function of time can be used to follow the rate of interaction of LAS with Ca^{++}. Calcium chloride was added to a 5.5×10^{-4} mol/l solution of LAS. Immediately after the addition of the calcium, the dynamic surface tension dropped sharply by more than seven erg/cm². The dynamic surface tension then increased gradually with time. The initial sharp reduction in the dynamic surface tension is a result of the sudden increase in electrolyte content which affected the packing of the surfactant at the surface. Given sufficient time, the LAS associates with the divalent calcium ions, resulting in a reduction in surfactant activity. These data demonstrate that the interaction between Ca^{++} and LAS is not instantaneous but requires a finite period of time. Instantaneous binding of calcium ions by a calcium binding detergent builder is not necessarilly a requirement for achieving satisfactory water hardness protection of LAS.

Figure 10 is a similar plot illustrating the effectiveness of several detergent builders for protecting LAS from calcium ions. The data were generated by first adding zeolite or sodium tripolyphosphate (STPP) to a 5.5×10^{-4} molar solution of LAS at ambient temperature followed by calcium addition in increments after the builders were dispersed or solubilized, as the case may be. The open symbols indicate that the solutions were clear, and the filled symbols indicate cloudy solutions.

The most effective builder for protecting LAS from Ca^{++} will accommodate the highest concentration of added Ca^{++} without showing a corresponding increase in surface tension. As shown in Figure 10, STPP accommodated slightly more Ca^{++} than zeolite A before the surface tension began to increase with increasing additions of Ca^{++}. The solution turned cloudy in the calcium concentration region from 1.35×10^{-3} mol/l to 1.6×10^{-3} mol/l. The turbid system observed at 1.6×10^{-3} mol/l calcium concentration had about the same effective concentration as that of the starting LAS solution, as indicated by the approximately 37 erg/cm² surface tension. As opposed to the STPP system, the presence of zeolite A did not reduce the dynamic surface tension of the LAS solution because zeolite A does not contribute to the ionic strength of the solution. The addition of calcium ions to the zeolite A/LAS sys-

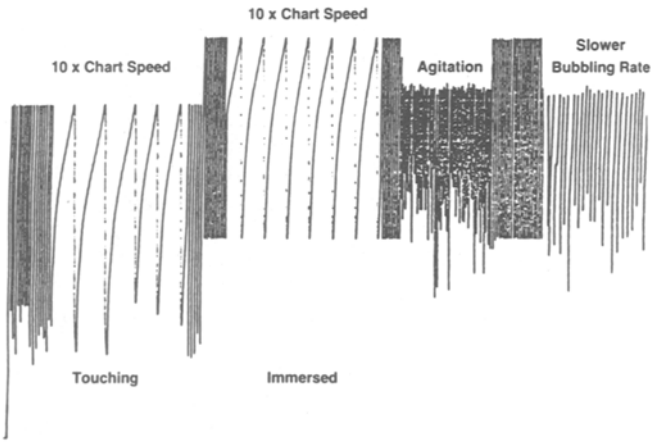

FIG. 8. Strip chart recording of dynamic surface tension measurement.

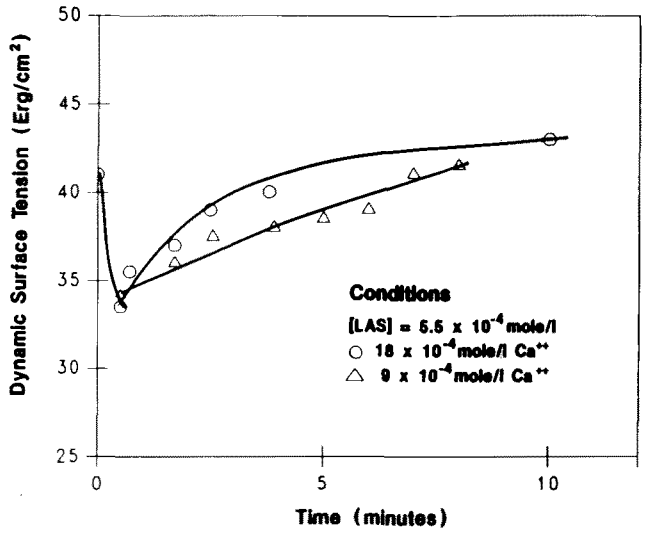

FIG. 9. Kinetics of LAS/CA^{++} interaction.

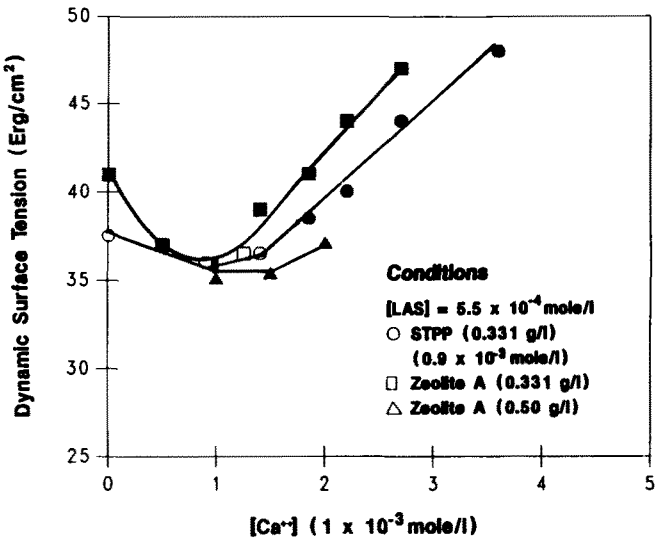

FIG. 10. Effectiveness of builders in protecting LAS from CA^{++}.

tem resulted in a larger decrease in the dynamic surface tension as a result of the replacement of two bound sodium ions by one calcium ion. At the same concentration of builder, the lowest dynamic surface tension occurred at about the same calcium concentration (9×10^{-4} mol/l) for both zeolite A and STPP. Increasing the zeolite concentration by 50% (from 0.331 g/l to 0.50 g/l) expanded the region of protection of the LAS from calcium ion interaction proportionately. These data show that the Ca^{++} binding rate of zeolite A is sufficient to prevent the interaction of LAS with calcium ions.

The data shown in Figure 11 were generated under conditions similar to those used for Figure 10 except that sodium citrate, sodium carbonate and Alcosperse™ 409N polyelectrolyte were used as the calcium binding agents. The Alcosperse™ 409N polyelectrolyte builder, provided by G.T. McGrew, Alco Chemical Corp., Chattanooga, Tennessee, is supplied in the acid form. The Alcosperse polymer was neutralized with sodium hydroxide before it was used. All the builders were used at a 0.331 g/l level on an active basis. The data show that pound for pound Alcosperse™ 409N polymer is more effective in protecting LAS from Ca^{++} interaction than sodium citrate which, in turn, is more effective than sodium carbonate.

Zeolite A is the only calcium binding builder widely used in the detergent industry that is water insoluble. This makes intimate contact between insoluble organic calcium salts and the ion exchange sites in zeolite virtually impossible, leading to speculations that zeolite, unlike soluble calcium binding builders, is not effective in solubilizing fatty organic salts. The data represented by Figure 12 illustrate the relative solubilization power of various detergent builders for insoluble organic calcium salts. A milky system containing 5.5×10^{-4} mol/l LAS and 9.0×10^{-4} mol/l calcium was aged at room temperature for at least 48 hr. At the beginning of an experiment, a calcium binding builder was added to the LAS/Ca^{++} solution and the dynamic surface tension measured at the three sec/bubble rate.

Upon addition of STPP to the aged LAS/Ca^{++} system, the dynamic surface tension dropped instantaneously and the milky solution turned clear. The addition of the same amount of zeolite A to a similar LAS/Ca^{++} system reduced the dynamic surface tension slowly, taking more than five min to reach a steady state. This demonstrates that the rate of $Ca(LAS)_2$ dissolution by zeolite A is slow. When a builder system consisting of one part by weight of STPP and three parts by weight zeolite A was added to the LAS/Ca^{++} system, the rate of dynamic surface tension lowering increased dramatically over that observed for just zeolite A and approached that observed for STPP alone. This demonstrates that use of a water soluble sequestering agent, such as STPP, provides a mechanism for increasing the rate of dissolution of insoluble organic calcium salts by zeolite A.

Figure 13 gives the results of a similar investigation using sodium carbonate and sodium citrate as the calcium binding agents. Figure 13 shows that the reduction in the dynamic surface tension in the LAS/Ca^{++} system as a result of the presence of either sodium carbonate or sodium citrate is very rapid. However, the absolute values of the dynamic surface ten-

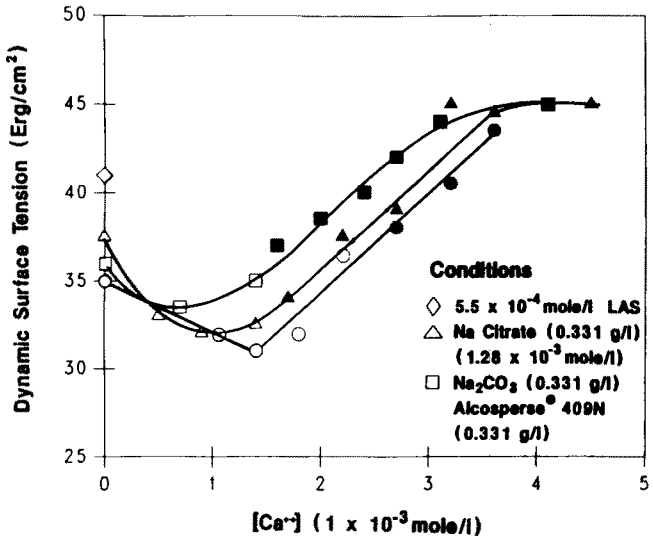

FIG. 11. Effectiveness of builders in protecting LAS from CA^{++}.

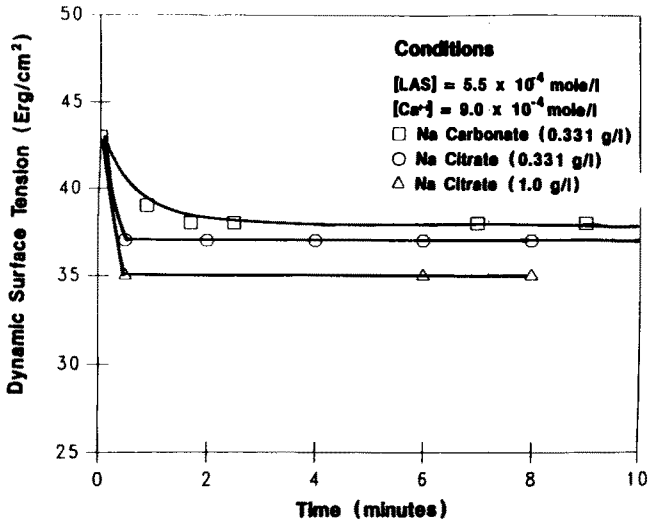

FIG. 12. Dissolution of Ca LAS by STPP, zeolite A and zeolite A/STPP.

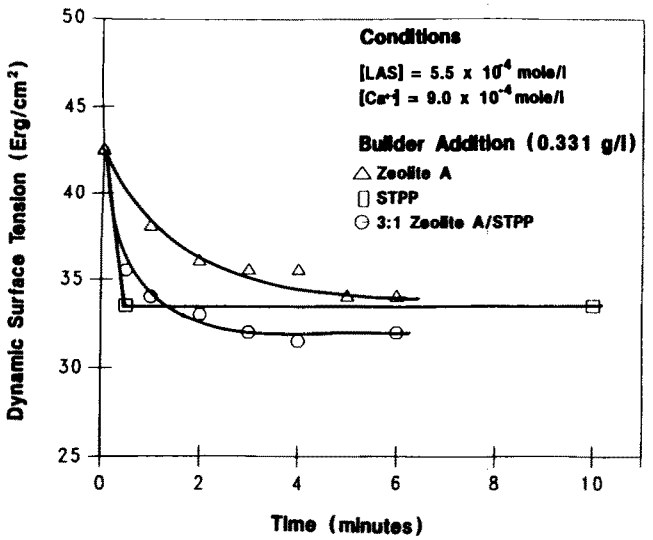

FIG. 13. Dissolution of Ca LAS by Na carbonate and Na citrate.

sion reductions achieved with sodium citrate and sodium carbonate are not as low as those achieved by using zeolite A or STPP.

REFERENCES

1. Hu, P.C., M.E. Tuvell and G.A. Bonner, SPE/DOE 12660, presented at the SPE/DOE Fourth Symposium on Enhanced Oil Recovery April, 1984.
2. Adamson, A.W., *Physical Chemistry of Surfaces*, 3rd edn., John Wiley & Sons, 1976, pg. 16
3. Mysels, K.J., *J. Phys. Chem. 86*:4648 (1982).
4. Prins, A., in *Foams*, edited by R.J. Akers, Academic Press, 1976, pp. 51-60.

[Received September 15, 1986; accepted March 1, 1988]